copyright by all rights reserved Quintessenz

FAM20A-Associated Amelogenesis Imperfecta: Gene Variants with Functional Verification and Histological Features

Jia Nan DING[1], Miao YU[1], Hao Chen LIU[1], Kai SUN[1], Jing WANG[2], Xiang Liang XU[2], Yang LIU[1], Dong HAN[1]

Objective: *To investigate FAM20A gene variants and histological features of amelogenesis imperfecta and to further explore the functional impact of these variants.*
Methods: *Whole-exome sequencing (WES) and Sanger sequencing were used to identify pathogenic gene variants in three Chinese families with amelogenesis imperfecta. Bioinformatics analysis, in vitro histological examinations and experiments were conducted to study the functional impact of gene variants, and the histological features of enamel, keratinised oral mucosa and dental follicle.*
Results: *The authors identified two nonsense variants c. 406C > T (p.Arg136*) and c.826C > T (p.Arg176*) in a compound heterozygous state in family 1, two novel frameshift variants c.936dupC (p.Val313Argfs*67) and c.1483dupC (p.Leu495Profs*44) in a compound heterozygous state in family 2, and a novel homozygous frameshift variant c.530_531insGGTC (p.Ser178Valfs*21) in family 3. The enamel structure was abnormal, and psammomatoid calcifications were identified in both the gingival mucosa and dental follicle. The bioinformatics and subcellular localisation analyses indicated these variants to be pathogenic. The secondary and tertiary structure analysis speculated that these five variants would cause structural damage to FAM20A protein.*
Conclusion: *The present results broaden the variant spectrum and clinical and histological findings of diseases associated with FAM20A, and provide useful information for future genetic counselling and functional investigation.*
Keywords: *amelogenesis imperfecta, FAM20A, frameshift variants, mutations, nonsense variants*
Chin J Dent Res 2024;27(1):53–63; doi: 10.3290/j.cjdr.b5136761

1 Department of Prosthodontics, Peking University School and Hospital of Stomatology & National Center for Stomatology & National Clinical Research Center for Oral Diseases & National Engineering Research Center of Oral Biomaterials and Digital Medical Devices, Beijing, P.R. China.
2 Department of Oral and Maxillofacial Surgery, Peking University School and Hospital of Stomatology & National Center for Stomatology & National Clinical Research Center for Oral Diseases & National Engineering Research Center of Oral Biomaterials and Digital Medical Devices, Beijing, P.R. China.

Corresponding authors: Dr Yang LIU and Dr Dong HAN, Department of Prosthodontics, Peking University School and Hospital of Stomatology, No. 22 Zhongguancun South Avenue, Haidian District, Beijing 100081, PR China. Tel: 86-10-82195393. Email: pkussliuyang@bjmu.edu.cn; donghan@bjmu.edu.cn

This study was supported by the National Natural Science Foundation of China (82270944, 82100976, and 81600846).

The teeth are one of the key parts of the stomatognathic system. The teeth, gingiva and periodontal tissue develop from tooth germ.[1] The tooth germ consists of three parts: the enamel organ, dental papilla and dental follicle.[2,3] The enamel organ is the epithelial part of the tooth germ[2], which gives rise to dental enamel and the epithelial part of the gingiva, whereas the dental papilla and dental follicle are the mesenchymal parts of the tooth germ.[4] The dental papilla develops into dental pulp and dentine, and the dental follicle forms cementum, periodontal ligament and alveolar bone.[5] Many genes participate in the development of tooth germ, and gene variants may lead to malformation of the teeth and adjacent tissue.[6-8]

Enamel is the hardest ectodermal tissue on the surface of the tooth crown.[9] The development of enamel

copyright by all rights reserved Quintessenz

involves two main processes[10]: matrix formation and mineralisation. Due to some gene variants, it may lead to changes in enamel matrix protein deposition and/or abnormal mineralisation[11], resulting in amelogenesis imperfecta (AI)12. According to the Witkop classification set out in 1988[13], AI was divided into four categories: hypoplastic (type I: OMIM#104530, OMIM#104500, OMIM#204650, OMIM#301200, OMIM#616270, OMIM#204690, OMIM#616221, OMIM#617297 and OMIM#620104;), hypomaturation (type II: OMIM#204700, OMIM#612529, OMIM#613211, OMIM#614832, OMIM#615887 and OMIM#617217), hypocalcified (type III: OMIM#130900, OMIM#617607 and OMIM#618386) and hypomaturation-hypoplastic with taurodontism (type IV: OMIM#104510).

FAM20A (OMIM * 611062) is one of the members of the FAM20 gene family (*FAM20A*, *FAM20B* and *FAM20C*) that encode kinases (phosphorylating enzymes) which modify proteins within the secretory pathway.[14] *FAM20A* gene located on human chromosome 17q24.2 consists of 11 exons and contains a highly conserved C-terminal domain.[15] FAM20A protein is considered to be a pseudokinase that forms a complex with FAM20C and allosterically activates FAM20C[15-18], thereby promoting phosphorylation of FAM20C targets.[19,20] FAM20A binds directly to FAM20C.[17] FAM20C protein is a Golgi casein kinase that phosphorylates the Ser-X-Glu/Ser(P) motif of most secretory proteins, including enamel matrix proteins.[21] FAM20C variants cause Raine syndrome[22], exhibiting bone and craniofacial/dental abnormalities.[17] FAM20B protein is a xylose kinase regulating proteoglycan synthesis.[19] *FAM20A* variant can lead to enamel hypoplasia (OMIM #204690)[23], which is inherited as autosomal recessive inheritance. This disease is also known as enamel-renal syndrome (ERS).[24] It is characterised by enamel hypoplasia, dental pulp stones, delayed eruption of permanent teeth, gingival overgrowth and renal calcinosis.[25]

In the present study, screening of the gene variants and histological and functional investigation were performed. Five variants of FAM20A were identified in three patients with AI, of which three were novel variants. The clinical phenotypes of the three probands were reported, and histological examinations revealed the dysplastic enamel structure and ectopic mineralisation in the dental follicle and gingival mucosa. The in vitro functional assay confirmed subcellular localisation changes and the functional impact of FAM20A variants.

Materials and methods

Pedigree construction and patient recruitment

All the probands and family members of three pedigrees requested treatment advice at the Department of Prosthodontics, Peking University School of Stomatology, Beijing, China. Oral examinations were carried out and panoramic dental radiographs were taken. Informed consent was obtained from all the participants. This study was approved by the Ethics Committee of Peking University School and Hospital of Stomatology (PKUSSIRB-202162021). A total of three nuclear families were recruited, all of whom denied consanguineous marriage. Three individuals were included in Sanger sequencing for each pedigree. Only the proband in each pedigree showed the enamel hypoplasia phenotype. The mode of inheritance was consistent with autosomal recessive inheritance.

Variant detection and analysis

Genomic DNA from these three probands of the three recruited pedigrees was isolated from peripheral blood lymphocytes using a BioTek DNA Whole-blood Mini Kit (BioTek, Beijing, China) according to the manufacturer's instructions. After polymerase chain reaction (PCR), DNA products were sheared to acquire 150- to 200-bp fragments. Whole-exome sequencing (WES) was performed by Beijing Angen Gene Medicine Technology (Beijing, China) with the Illumina-X10 platform. After this, the detected variants were filtered according to the following methods. Firstly, all genes associated with tooth development were analysed[26,27], especially for AI-associated genes. Secondly, non-synonymous single nucleotide variants (SNVs) and insertions/deletions (InDels) with a minor allele frequency (MAF) ≥ 0.01 in bioinformatic databases, including the single nucleotide polymorphism database (dbSNP, http://www.ncbi.nlm.nih.gov/projects/SNP/snpsummary.cgi), the Genome Aggregation Database (gnomAD, http://gnomad.broadinstitute.org), the Human Gene Mutation Database (HGMD, http://www.hgmd.org) and the 1,000 Genomes Project data in Ensembl (http://asia.ensembl.org/Homo_sapiens/Info/Index) were excluded. Finally, pathogenicity of the remaining variants was further predicted using the Protein Variation Effect Analyzer (PROVEAN, https://www.jcvi.org/research/provean) and polymorphism phenotyping (PolyPhen-2, http://genetics.bwh.harvard.edu/pph2/).

copyright by all rights reserved Quintessenz

Sanger sequencing and clone sequencing

Variants of *FAM20A* (NM_017565.4) were identified in three affected families. Co-segregation analysis and Sanger sequencing of the probands and their family members were performed to verify the variants of *FAM20A* based on WES results.

For further verification, the related *FAM20A* (NM_017565.4) fragments were sequenced using Sanger sequencing. Genomic DNA from these family members was isolated according to the procedure described above. We designed the corresponding primers (provided on request) for each variant. The PCR products were sequenced by Ruibio Biotech (Beijing, China). TA clone sequencing was used to confirm the exact status of the frameshift and nonsense variants.

Bioinformatics

To carry out the bioinformatics analysis, we also used a series of bioinformatics databases, such as MutationTaster (https://www.mutationtaster.org/) and PROVEAN. The pathogenicity of the three variants was classified according to the American College of Medical Genetics and Genomics (ACMG) guideline.[28]

The secondary structure of wild-type FAM20A and five mutated variants was predicted using PsiPred 4.0 (http://bioinf.cs.ucl.ac.uk/psipred). An optimum template of FAM20A protein was selected for homology modelling analysis through SWISS-MODEL (https://swiss-model.expasy.org) and the tertiary structural changes of variants were captured using PyMOL software (Molecular Graphics System, DeLano Scientific, San Carlos CA, USA).

Scanning electron microscope (SEM) examination of the affected teeth

Teeth 25,16 and 65 were extracted from proband 302, then fixed in 10% neutral formaldehyde solution. Tooth 65 was separated to expose the inner surface, then the pieces were etched with 30% phosphate gel, rinsed with distilled water thoroughly and dried in the vacuum drying oven at 37°C overnight. After being coated with gold, the teeth samples were observed under a scanning electron microscope.

Hematoxylin-eosin (HE) staining of the patient's gingival mucosa and dental follicle

A small piece of gingival mucosa was obtained during patient 302's oral surgery. The dental follicle was obtained during the extraction of impacted tooth 16. The samples were fixed in 10% neutral formaldehyde solution at room temperature for 24 hours, then embedded in paraffin and mounted on the slicing machine and sectioned to a thickness of 5 μm. The sections were stained with hematoxylin and eosin following the routine process and observed under the microscope.

Construction of plasmids

The full-length coding region of the human FAM20A gene (NM_017565.4) was cloned into the pEGFP-C1 expression vector with enhanced GFP to synthesise the wild-type plasmid pEGFP-C1-FAM20A. Then, in vitro site-directed mutagenesis was performed to generate five mutated plasmids: pEGFP-C1-R136X, pEGFP-C1-S178Vfs*21, pEGFP-C1-R276X, pEGFP-C1-V313Rfs*67 and pEGFP-C1-L495Pfs*44. All plasmids were synthesised by Ruibio Biotech, and the company also confirmed the entire sequence of the mutated constructs.

Cell culture and transfection

Human embryonic kidney 293T cells were cultured in Dulbecco's modified Eagle medium (Invitrogen, Waltham, MA, USA) supplemented with 10% foetal bovine serum and 2 mmol/L L-glutamine in the presence of 5% CO_2. Following the manufacturer's instructions, transient transfection was carried out using Lipofectamine 3000 (Invitrogen).

Subcellular localisation assay

We transiently transfected 293T cells with pEGFP-C1 expression plasmids containing GFP-wild-type or mutated FAM20A cDNA fusion proteins. At 48 hours after transfection, the cells were washed three times with phosphate buffer and fixed with 4% paraformaldehyde for 15 minutes. After washing, the cells were placed in a mounting medium with 4',6-diamidino-2-phenylindole (Solarbio, Beijing, China), mounted and photographed using an LSM 510 Meta confocal microscope (Zeiss, Oberkochen, Germany) with a ×63/1.00 numerical aperture oil objective lens.

Co-immunoprecipitation (Co-IP) and immunoblotting

Human embryonic kidney 293T (HEK-293T) cells were transiently co-transfected with the GFP empty vector, wild-type mutant FAM20A-GFP and wild-type FAM20C-FLAG plasmids using Lipofectamine 3000. Proteins from each group were harvested 48 hours after co-transfection.

copyright by all rights reserved Quintessenz

50 µl of each protein sample was removed as input. GFP-Trap Magnetic Agarose (gtma, Chromotek, Germany) were pre-treated according to the manufacturer's instructions and added to the other protein supernatants obtained overnight at 4°C. The next day, the beads were washed until the supernatant was clear. The washed beads were resuspended in 2× SDS sample buffer and the supernatant was the IB group. To observe the protein expression, the IB and input samples were assessed through Western blot analysis. After electrophoresis on 10% polyacrylamide gel, the protein was transferred to a PVDF membrane by electrophoresis and then incubated with anti-GFP (ab1218) mouse antibody (Abcam, Cambridge, UK) and anti-Flag (AE092) rabbit antibody (Abclonal, Wuhan, China). The membrane was washed and incubated with peroxidase-conjugate rabbit or mouse anti-mouse secondary antibodies (ab150077, Abcam; ab6728, Abcam).

Results

Clinical findings confirmed AI and eruption defect

The dental characteristics and panoramic radiographs of the probands are shown in Fig 1. In family 1, the proband (302) was a 19-year-old woman. Intraoral photographs showed mixed dentition, small dental crowns with generally thin enamel and yellow discolouration of teeth (Fig 1a to c). Obviously, her occlusal vertical distance was decreased. Radiographic examination revealed impacted permanent teeth with enamel defect (Fig 1d). The roots of all her teeth were generally short. Her parents both had normal enamel without any disorder. The proband stated that she had been diagnosed as having bilateral medullary nephrosis with small calcifications in both kidneys.

In family 2, the proband (748) was a 24-year-old woman. She had completed most of her dental crown restorations at another hospital when the intraoral pictures were taken. Only teeth 17, 35 and 36 without restoration revealed the original appearance of thin enamel (Fig 1e and f). Radiographic film taken prior to restoration showed no radiopaque enamel, delayed tooth eruption and intrapulpal calcifications (Fig 1g). Unfortunately, her parents had passed away. Her two brothers had normal teeth and well-developed enamel.

In family 3, the proband (914) was a 15-year-old boy. An intraoral scan was taken using a TRIOS intraoral scanner (3Shape, Copenhagen, Denmark). In addition to thin enamel, he also showed an anterior open bite, which may have been caused by an eruption defect and decreased occlusal vertical distance (Fig 1h to j). The panoramic radiograph showed that he had short roots and impacted teeth (Fig 1k). His parents both had normal dentition.

Notably, as seen on the panoramic radiographs taken of all three patients, the impacted teeth showed enamel defects as well.

Sequencing of patients and family members detected FAM20A variants

The pedigree of three family lines is shown in Fig 2a to c. Using whole-exome sequencing (WES), we identified five variants of the *FAM20A* gene in these families and confirmed them through Sanger sequencing (Fig 2d to h). The two nonsense variants had been documented previously, whereas three frameshift variants were novel, then a pathogenicity prediction was made for all variants (Table 1).

In family 1, proband 302 carried *FAM20A* compound heterozygous variants c.406C > T (p.Arg136*) and c. 826C > T (p.Arg276*). Her father only carried the heterozygous nonsense variant c.406C > T (p.Arg136*), while her mother only carried another heterozygous nonsense variant c. 826C > T (p.Arg276*). According to family co-segregation, the variants of the proband were inherited from both her parents through an autosomal-recessive mode of inheritance.

In family 2, proband 748 carried *FAM20A* compound heterozygous variants c.936dupC (p.Val313Argfs*67) and c.1483dupC (p.Leu495Profs*44). Unfortunately, both of her parents had passed away and were unavailable for genetic screening. Her two brothers were both heterozygous, carrying the frameshift variant c.936dupC (p.Val313Argfs*67), and had normal dentition, which was in accordance with the autosomal-recessive mode.

In family 3, proband 914 carried a *FAM20A* homozygous variant c.530_531insGGTC (p.Ser178Valfs*21). His parents both carried the same heterozygous variant. His family co-segregation also revealed an autosomal-recessive inheritance pattern.

Bioinformatics analysis indicated functional impact of FAM20A variants

To predict the functional impact of these variants, we first searched the dbSNP and gnomAD databases, then carried out pathogenicity prediction using PROVEAN and MutationTaster. We then classified these nonsense and frameshift variants as pathogenic variants according to the ACMG classification (Table 1).

By predicting the secondary structure of FAM20A protein, it can be found that all the nonsense and

copyright by all rights reserved Quintessenz

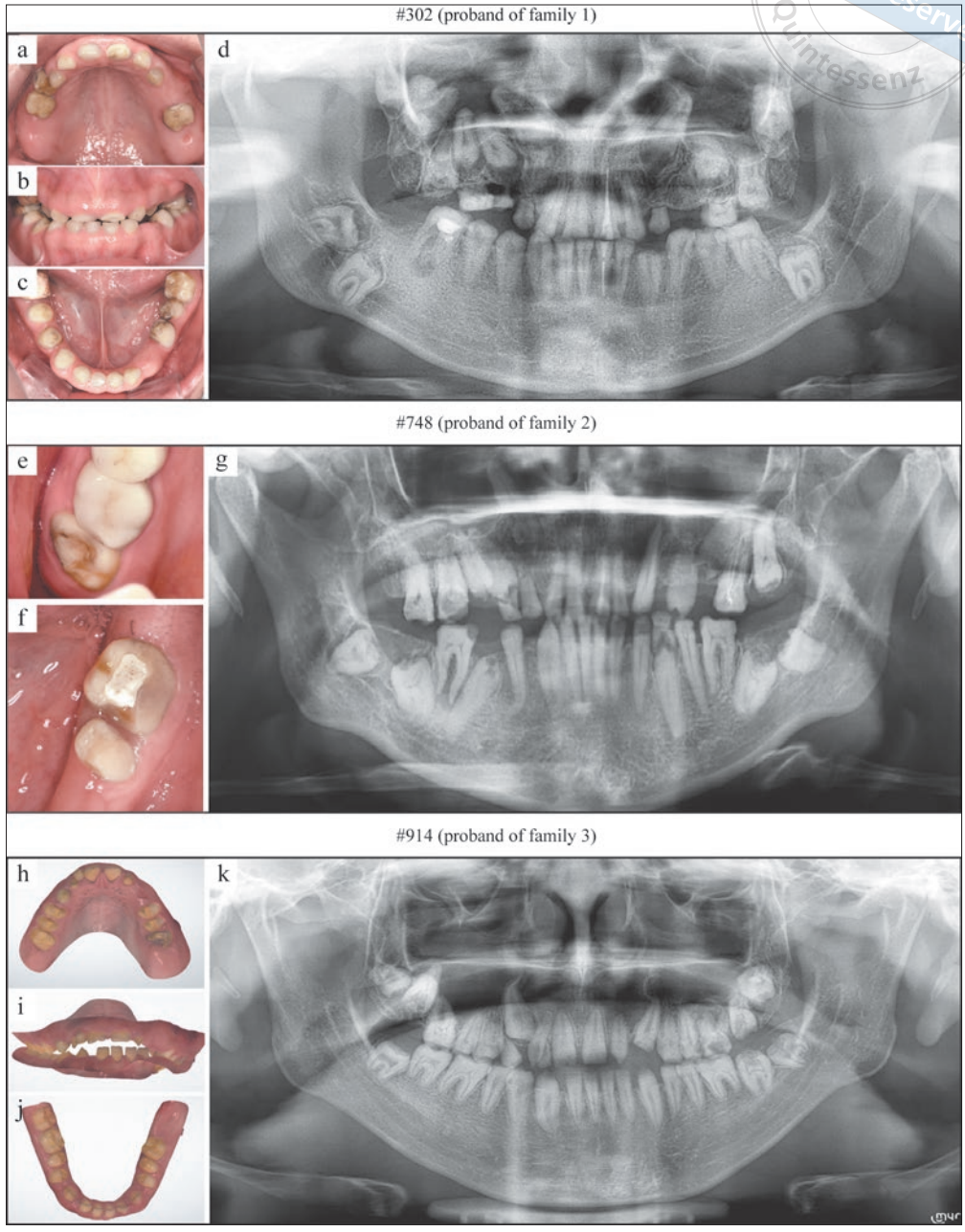

Fig 1 Dental characteristics of the three patients. Digital photographs and panoramic radiograph of proband 302 **(a to d)** and proband 748 **(e to g)**. Intraoral scan images and panoramic radiograph of proband #914 **(h to k)**.

frameshift variants lead to the truncation of the normal protein, resulting in serious changes to the structure of FAM20A. The tertiary protein structure analysis also shows that the proteins are truncated and the spatial structures have changed (Fig 3).

Histomorphological analyses of the clinical samples confirmed the enamel defect and ectopic mineralisation in the mucosa and dental follicle

Three teeth were obtained from proband 302, including unerupted 25, unerupted 16 and erupted 65 with heavy abrasion. The root morphology of tooth 16 was irregular and curved, and a developmental anomaly could be seen near the apex (Fig 4a). Tooth 65 was divided into two halves according to the buccolingual direction. Calcification of the pulp cavity was notable, and the enamel could hardly be seen on the tooth (Fig 4b).

SEM analysis of the surface of tooth 25 (Fig 4c and e) revealed a variety of features, including rough, knob-like calcifications and some relatively smooth mineral. SEM analysis of the occlusal surface of tooth 65 (Fig 4d and f) showed some larger craters suggestive of resorption lacunae.

copyright by all rights reserved Quintessenz

Table 1 Summary of FAM20A variants in the present study.

Family	Exon	Nucleotide change	Protein change	Variation type	dbSNP (AF)	gnomAD (MAF)	Provean	Mutation Taster	ACMG classification (evidence of pathogenicity)
Family1	2	c.406C>T	p.R136*	Nonsense	rs144411158 (0.000000)	0.000003979	Neutral	Disease-causing	PVS1+PS3+PM2+PM4+ PP1+PP4+PP5
									Pathogenic
Family1	6	c.826C>T	p.R276*	Nonsense	rs387907215 (0.00000)	––	Deleteri-ous	Disease-causing	PVS1+PS3+PM2+PM4+ PP1+PP4+PP5
									Pathogenic
Family2	11	c.1483dupC	p.L495Pfs*44	Frameshift	/	––	/	Disease-causing	PVS1+PS3+PM2+PM4+ PP1+PP4
									Pathogenic
Family2	7	c.936dupC	p.V313Rfs*67	Frameshift	/	––	/	Disease-causing	PVS1+PM2+PM4+PP1+PP4
									Pathogenic
Family3	2	c.530_531insGGTC	p.S178Vfs*21	Frameshift	/	––	/	Disease-causing	PVS1+PS3+PM2+PM4+ PP1+PP4
									Pathogenic

—, Variant was not found in ExAC; /, Variant cannot be predicated in dbSNP or Provean.

A small piece of the oral gingival mucosa and the dental follicle were obtained from proband 302. Upon HE staining, they both presented ectopic psammomatoid calcifications (Fig 4g and h).

In vitro experiments revealed changes in subcellular localisation of FAM20A variants

To evaluate the subcellular localisation of the FAM20A variants, we determined the subcellular localisation of the five mutated proteins by immunofluorescence. The results showed that wild-type FAM20A was located in the cytoplasm, but the localisation of the FAM20A variants R136*, R276*, L495Pfs*44 and S178Vfs*21 was altered. GFP-R136*, GFP-R276* and GFP-S178Vfs*21 were located in the whole cytoplasm with weak expression in the nucleus (Fig 5c-c", d-d" and e-e"). Notably, GFP-L495Pfs*44 was scattered in the nucleus and densely clumped in the nucleolus (Fig 5g-g"), which was very different from the wild-type. The results indicated that R136*, R276*, L495Pfs*44 and S178Vfs*21 severely affected the subcellular localisation of FAM20A, which might contribute to the pathogenic process in these patients. On the other hand, the V313Rfs*67 variant seemed to be located in the same place in the cell as the wild type (Fig 5f-f"), but without local condensation in the cytoplasm, suggesting that the V313Rfs*67 may lead to developmental anomalies in a different way compared with the other four variants.

Co-immunoprecipitation (Co-IP) and immunoblotting illustrate reduced binding of mutant FAM20A protein to FAM20C

Based on the results, FAM20A protein is shown to have the ability to bind to FAM20C protein in vitro. The five mutants also have a weakened binding tendency compared to the wild-type (Fig 6). The molecular weights of the mutant proteins were all reduced to varying degrees, further supporting the aforementioned predictions for the proteins; however, no comparisons were made between the variants to determine the severity of the reduction in binding capacity.

Discussion

AI generally refers to inherited enamel malformations that may include other local defects such as delayed tooth eruption and misshapen roots.[24,29] In the case of enamel-renal syndrome (ERS)[25], the dental problems may appear prior to any evidence of kidney disease, perhaps because kidney ultrasound examinations are rarely performed on AI patients. Proband 302 in family 1 described herself as having bilateral medullary nephrosis with small calcifications in both kidneys, but did not provide the results of her renal examination. For patients diagnosed with bi-allelic *FAM20A* variants, it is advisable that the kidney be examined regularly to achieve early diagnosis and treatment. The proband of family 1 carried *FAM20A* complex heterozygous variants c.406C > T (p.Arg136*) and c.826C > T(p.Arg276*). Although these two nonsense variants have been pre-

copyright by all rights reserved Quintessenz

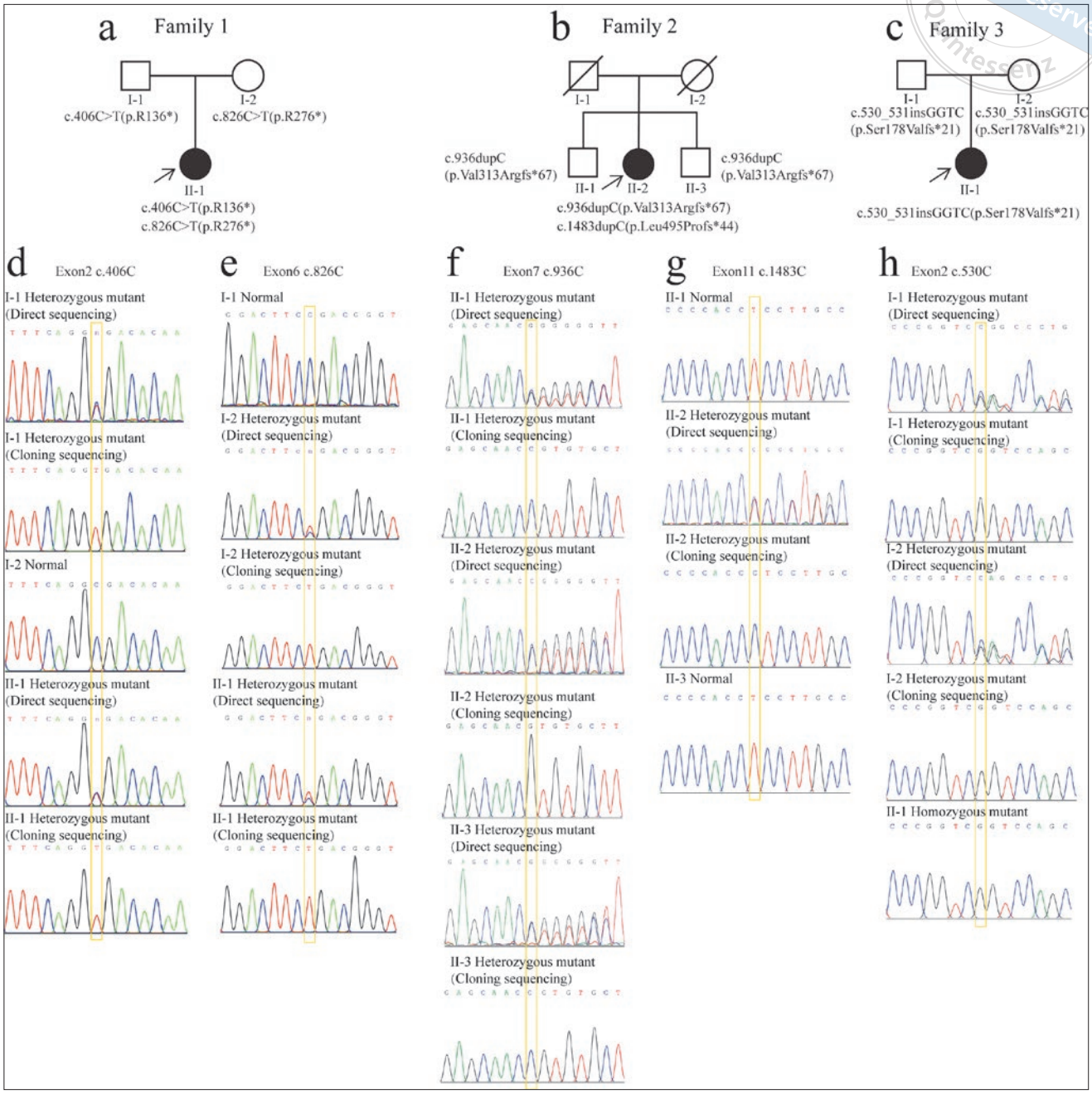

Fig 2 Pedigree and sequencing chromatograms of the three families. Pedigree of family 1 **(a)**, family 2 **(b)** and family 3 **(c)**. DNA sequencing chromatogram showing a heterozygous *FAM20A* variant of c.406C > T (p.Arg136*) in proband 302 (II-1) and her father (I-1) **(d)**. DNA sequencing chromatogram showing a heterozygous *FAM20A* variant of c. 826C > T (p.Arg276*) in proband 302 (II-1) and her mother (I-2) **(e)**. DNA sequencing chromatogram showing a heterozygous *FAM20A* variant of c.936dupC (p.Val313Argfs*67) in proband 748 (II-2) and her two brothers (I-1, II-3) **(f)**. DNA sequencing chromatogram showing a heterozygous *FAM20A* variant of c.1483dupC (p.Leu495Profs*44) in proband 748 (II-2) **(g)**. DNA sequencing chromatogram showing a homozygous *FAM20A* variant of c.530_531insGGTC (p.Ser178Valfs*21) in proband 914 (II-2) and the same heterozygous FAM20A variant in his parents (I-1, I-2) **(h)**.

copyright by all rights reserved

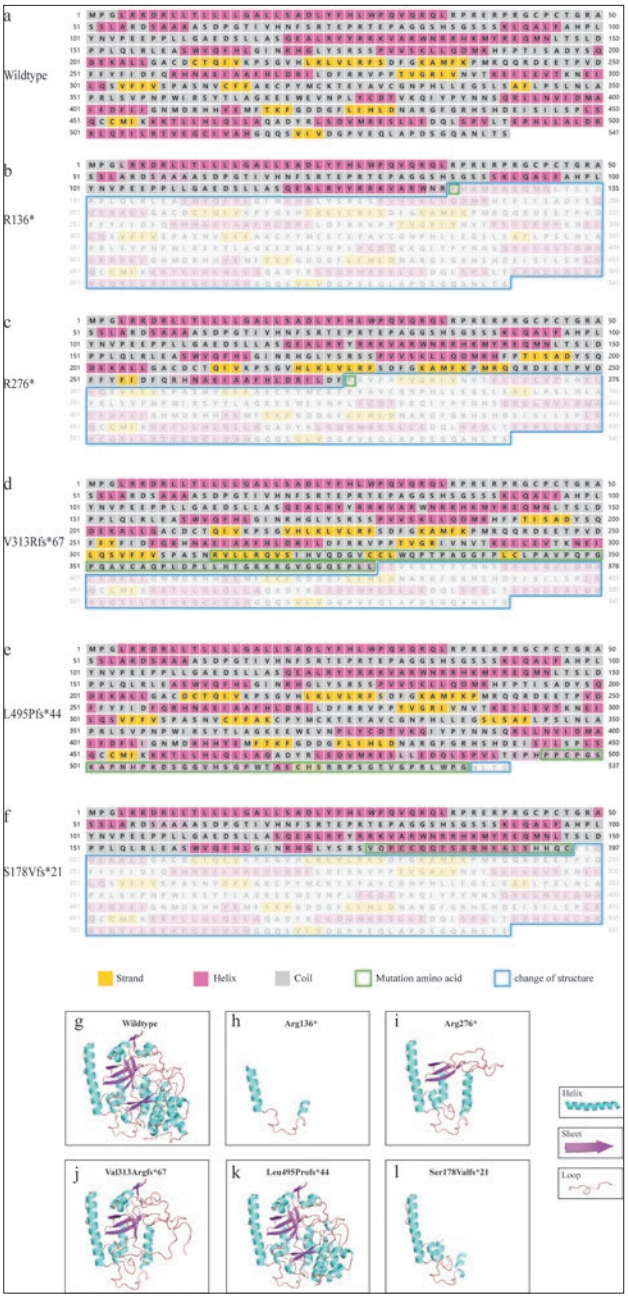

Fig 3 Bioinformatics analysis of the FAM20A variants. The predicted secondary structure of the wild-type FAM20A protein **(a)**. The predicted secondary structure of five mutated FAM20A proteins. Sites of variants are indicated by green squares. The structural changes in these mutated proteins compared to the wild-type FAM20A are shown as blue squares, α-Helices are represented as pink squares, strands are represented as yellow squares, and while coils are represented as grey squares **(b to f)**. Tertiary structural modelling of the FAM20A protein **(g)**. Predicted tertiary structural changes in the five altered proteins **(h to l)**.

viously reported separately in compound heterozygous states with other variants[22,30], in the present study their presence in the compound heterozygous state is novel. We found that the root development of the unerupted molar was abnormal and the root apex of tooth 16 was curved, which was consistent with previous literature.[25] SEM analysis revealed a rough calcified nodule area and a relatively smooth mineral area on the crown surface, which was consistent with previous literature.[25] Through HE staining, the dental follicle and gingival mucosa of proband 302 displayed psammomatoid calcifications, and the ectopic mineralisation in the dental follicle and gingival mucosa was in accordance with previous literature.[23,24] This reoccurrence of clinical findings from different studies further confirmed the phenotypes related with FAM20A variants.

Proband 748 from family 2 carried FAM20A complex heterozygous variants c.936dupC (p.Val313Argfs*67) and c.1483dupC (p.Leu495Profs*44). These are both novel variants that have not been reported before, and both of which lead to truncation of the protein and functional impairment of FAM20A protein. Interestingly, variant Leu495Profs*44 is changed from the 495th amino acid near the end of the protein, while wildtype FAM20A has 541 amino acids. However, the change in its intracellular localisation was the most significant among the five variants found in the present study. The Leu495Profs*44 variant is restricted densely in the nucleolus. An intact signal sequence is necessary for secretion of FAM20A and that secretion is accompanied by prominent localisation of the protein to the ER.[14] If the highly conserved C-terminal putative kinase domain of FAM20A is mutated, the original signal sequence is lost, which may lead to re-entry from the endoplasmic reticulum into the nucleus.[14] The variant Leu495Profs*44 is predicted to disrupt the signal sequence without grossly altering the other structure. The subcellular localisation results of the present study confirmed the structure prediction, and this result provided new evidence for the function of FAM20A subdomains.

Proband 914 carried a FAM20A homozygous variant, c.530_531insGGTC (p.Ser178Valfs*21), which was novel and led to severe protein truncation. His parents both carried the rare heterozygous variant, but denied consanguineous marriage. He showed anterior open bite, which could be attributed to the eruption disorder related to FAM20A variant. This speculation needs to be confirmed further with future clinical and functional studies.

Based on the Co-IP results, we can see that all five variants weaken the ability to bind to FAM20C, affecting

copyright by all rights reserved

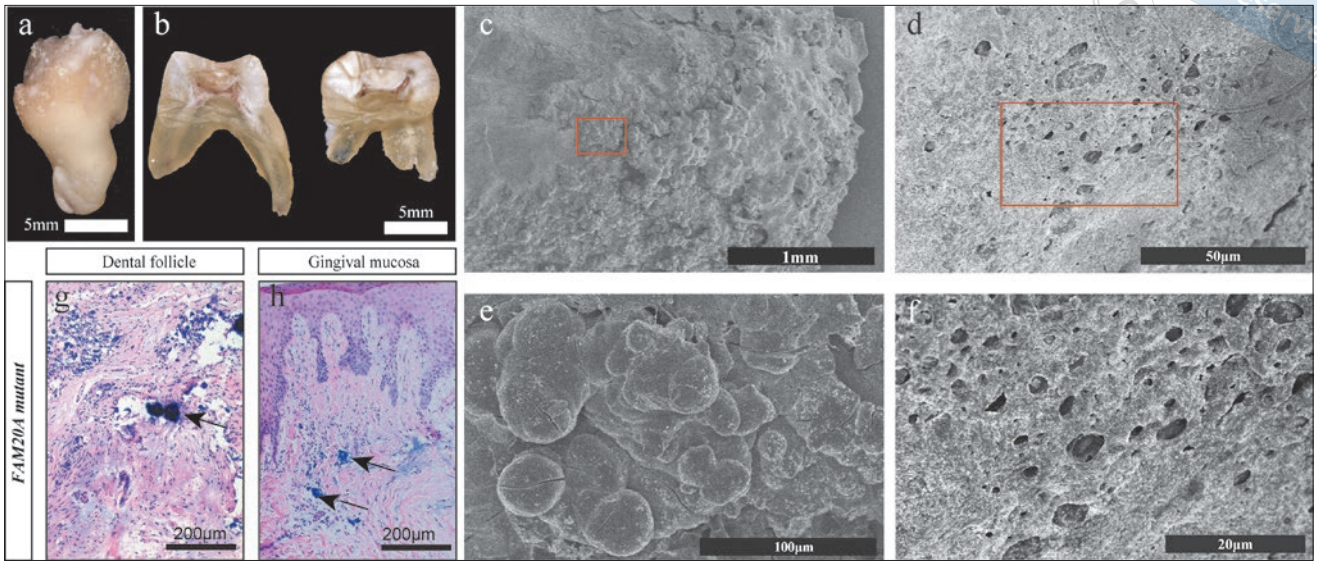

Fig 4 Histological features of proband 302's teeth, dental follicle and gingival mucosa. Photograph of tooth 16 **(a)**. Photograph of tooth 16 shows curved roots and poorly developed root morphology (b). Photograph of tooth 65 cut in a buccolingual direction with thin enamel **(c)**. Low magnification view of the occlusal surface of tooth 65 for SEM analysis **(d)**. Higher magnification of the box in panel c **(e)**. Higher magnification of the box in panel d **(f)**. HE section showing dental follicle tissue, with the arrow indicating ectopic psammomatoid calcification **(g)**. HE section showing gingiva mucosa, arrows indicating ectopic psammomatoid calcification **(h)**.

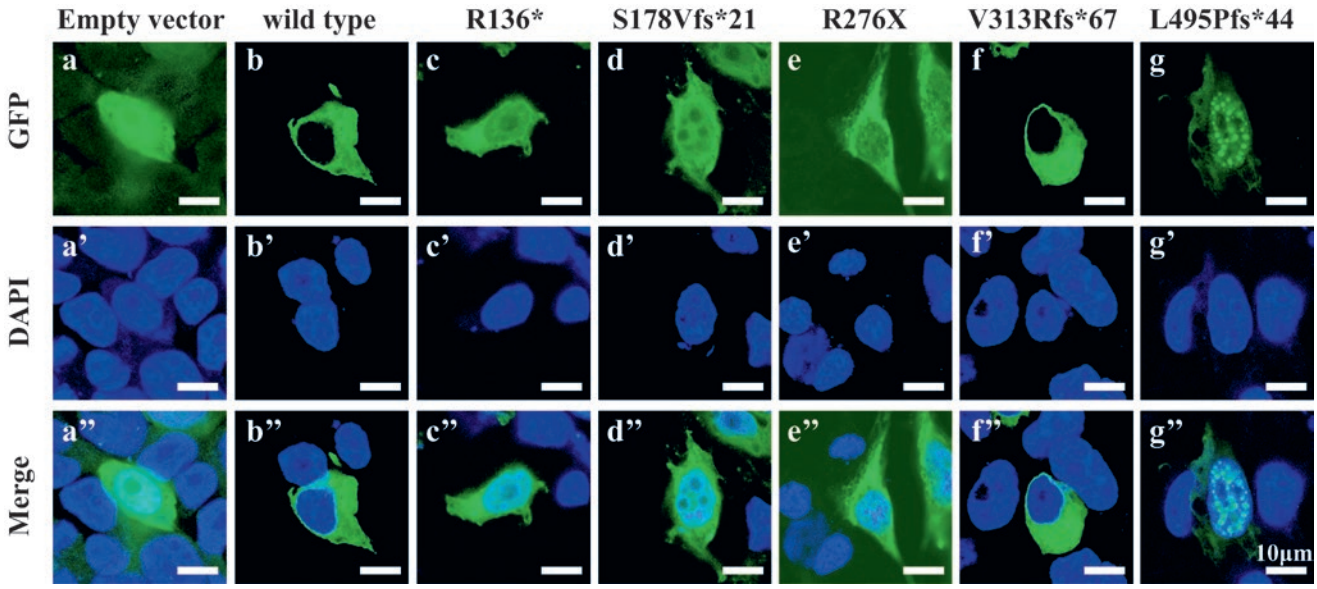

Fig 5 Expression and subcellular localisation of wild-type and mutated FAM20A proteins. Subcellular localisation of wild-type or mutated FAM20A. Cells transfected with GFP-R136*, GFP-R276* and GFP-S178Vfs*21 show expression in the entire cytoplasm with weak expression in the nucleus. GFP-V313Rfs*67 is located in the same location as the wild type, yet without local condensation in the cytoplasm. GFP-L495Pfs*44 shows densely clumped distributions within the nucleus. The empty vector with GFP was transfected into 293T cells as a negative control **(a to g)**. Nuclei staining by DAPI, 4,6-diamino-2-phenylindole **(a' to g')**. Merge of GFP and DAPI **(a" to g")**. FAM20A (GFP, green); nuclei (DAPI, blue)

copyright by all rights reserved Quintessenz

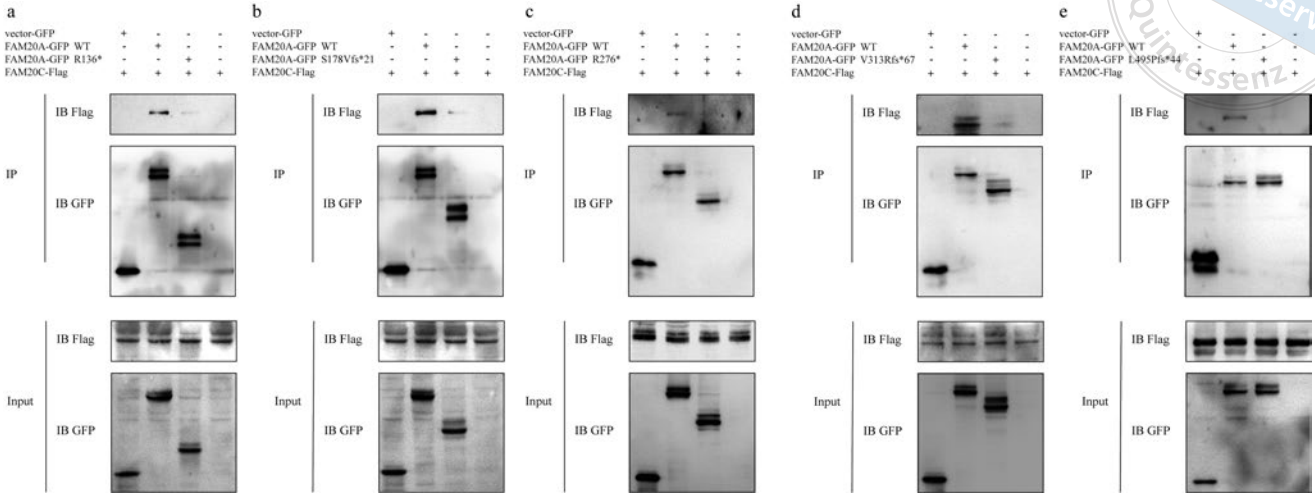

Fig 6 Co-immunoprecipitation of the variants. FAM20A variant R136* has a reduced ability to bind to FAM20C **(a)**. FAM20A variant S178Vfs*21 has a reduced ability to bind to FAM20C **(b)**. FAM20A variant R276* has a reduced ability to bind to FAM20C **(c)**. FAM20A variant V313Rfs*67 has a reduced ability to bind to FAM20C **(d)**. FAM20A variant L495Pfs*44* has a reduced ability to bind to FAM20C **(e)**.

the downstream function of the FAM20A-FAM20C complex, which leads to the development of AI. The present findings are also consistent with those from previous literature.[18,25]

Conclusion

The present authors identified five *FAM20A* variants, three of which were novel, in three patients with AI, and verified the functional impacts with in vitro experiments. The clinical and histological features were also recorded. This study broadened the variant spectrum of *FAM20A* and will facilitate in-depth investigation in the future.

Conflicts of interest

The authors declare no conflicts of interest related to this study.

Author contribution

Dr Jia Nan DING contributed to the data acquisition, analysis, interpretation and manuscript draft; Drs Miao YU, Hao Chen LIU and Kai SUN contributed to the data acquisition and interpretation; Drs Jing WANG and Xiang Liang XU assisted in the experiments; Dr Yang LIU contributed to the study design and manuscript draft and critical revision; Dr Dong HAN contributed to the conception and critical revision of the manuscript; All authors gave final approval for the manuscript.

(Received Jun 30, 2023; accepted Nov 23, 2023)

References

1. He XY, Sun K, Xu RS, et al. Spatial signalling mediated by the transforming growth factor-β signalling pathway during tooth formation. Int J Oral Sci 2016;8:199–204.
2. Xiong Y, Fang Y, Qian Y, et al. Wnt production in dental epithelium is crucial for tooth differentiation. J Dent Res 2019;98:580–588.
3. Tziafas D, Kodonas K. Differentiation potential of dental papilla, dental pulp, and apical papilla progenitor cells. J Endod 2010;36:781–789.
4. Mahdee AF, Ali AH, Gillespie JI. Structural and functional relations between the connective tissue and epithelium of enamel organ and their role during enamel maturation. J Mol Histol 2021;52:975–989.
5. Zeng L, He H, Sun M, et al. Runx2 and Nell-1 in dental follicle progenitor cells regulate bone remodeling and tooth eruption. Stem Cell Res Ther 2022;13:486.
6. Wang H, Pan M, Ni J, et al. ClC-7 deficiency impairs tooth development and eruption. Sci Rep 2016;6:19971.
7. Mitsui SN, Yasue A, Masuda K, et al. Novel PAX9 mutations cause non-syndromic tooth agenesis. J Dent Res 2014;93:245–249.
8. Brook AH. Multilevel complex interactions between genetic, epigenetic and environmental factors in the aetiology of anomalies of dental development. Arch Oral Biol 2009;54 (suppl 1):S3–S17.
9. de la Dure-Molla M, Quentric M, Yamaguti PM, et al. Pathognomonic oral profile of enamel renal syndrome (ERS) caused by recessive FAM20A mutations. Orphanet J Rare Dis 2014;9:84.
10. Robinson C, Kirkham J, Brookes SJ, Bonass WA, Shore RC. The chemistry of enamel development. Int J Dev Biol 1995;39:145–152.

copyright by all rights reserved Quintessenz

11. Li L, Saiyin W, Zhang H, et al. FAM20A is essential for amelogenesis, but is dispensable for dentinogenesis. J Mol Histol 2019;50:581–591.
12. Suchancova B, Holly D, Janska M, et al. Amelogenesis imperfecta and the treatment plan - Interdisciplinary team approach. Bratisl Lek Listy 2014;115:44–48.
13. Witkop CJ Jr. Amelogenesis imperfecta, dentinogenesis imperfecta and dentin dysplasia revisited: problems in classification. J Oral Pathol 1988;17:547–553.
14. Nalbant D, Youn H, Nalbant SI, et al. FAM20: An evolutionarily conserved family of secreted proteins expressed in hematopoietic cells. BMC Genomics 2005;6:11.
15. Cui J, Zhu Q, Zhang H, et al. Structure of Fam20A reveals a pseudokinase featuring a unique disulfide pattern and inverted ATP-binding. Elife 2017;6:e23990.
16. Wang SK, Reid BM, Dugan SL, et al. FAM20A mutations associated with enamel renal syndrome. J Dent Res 2014;93:42–48.
17. Ohyama Y, Lin JH, Govitvattana N, et al. FAM20A binds to and regulates FAM20C localization. Sci Rep 2016;6:27784.
18. Wang SK, Zhang H, Wang YL, et al. FAM20A mutations and transcriptome analyses of dental pulp tissues of enamel renal syndrome. Int Endod J 2023;56:943–954.
19. Zhang H, Zhu Q, Cui J, et al. Structure and evolution of the Fam20 kinases. Nat Commun 2018;9:1218.
20. Worby CA, Mayfield JE, Pollak AJ, et al. The ABCs of the atypical Fam20 secretory pathway kinases. J Biol Chem 2021;296:100267.
21. Zuo H, Yang D, Wan Y. Fam20C regulates bone resorption and breast cancer bone metastasis through Osteopontin and BMP4. Cancer Res 2021;81:5242–5254.
22. Hung CY, Rodriguez M, Roberts A, Bauer M, Mihalek I, Bodamer O. A novel FAM20C mutation causes a rare form of neonatal lethal Raine syndrome. Am J Med Genet A 2019;179:1866–1871.
23. Simancas Escorcia V, Diarra A, Naveau A, et al. Lack of FAM20A, ectopic gingival mineralization and chondro/osteogenic modifications in enamel renal syndrome. Front Cell Dev Biol 2020;8:605084.
24. Dourado MR, Dos Santos CRR, Dumitriu S, et al. Enamel renal syndrome: A novel homozygous FAM20A founder mutation in 5 new Brazilian families. Eur J Med Genet 2019;62:103561.
25. Wang SK, Aref P, Hu Y, et al. FAM20A mutations can cause enamel-renal syndrome (ERS). PLoS Genet 2013;9:e1003302.
26. Prasad MK, Geoffroy V, Vicaire S, et al. A targeted next-generation sequencing assay for the molecular diagnosis of genetic disorders with orodental involvement. J Med Genet 2016;53:98–110.
27. Rey T, Tarabeux J, Gerard B, et al. Protocol GenoDENT: Implementation of a new NGS panel for molecular diagnosis of genetic disorders with orodental involvement. Methods Mol Biol 2019;1922:407–452.
28. Richards S, Aziz N, Bale S, et al. Standards and guidelines for the interpretation of sequence variants: A joint consensus recommendation of the American College of Medical Genetics and Genomics and the Association for Molecular Pathology. Genet Med 2015;17:405–424.
29. Kantaputra PN, Bongkochwilawan C, Lubinsky M, et al. Periodontal disease and FAM20A mutations. J Hum Genet 2017;62:679–686.
30. Cho SH, Seymen F, Lee KE, et al. Novel FAM20A mutations in hypoplastic amelogenesis imperfecta. Hum Mutat 2012;33:91–94.